



Original Full Length Article

Mixed-mode toughness of human cortical bone containing a longitudinal crack in far-field compression

Diana Olvera^a, Elizabeth A. Zimmermann^{a,b}, Robert O. Ritchie^{a,b,*}^a Materials Sciences Division, Lawrence Berkeley National Laboratory, Berkeley, CA 94720, USA^b Department of Materials Science and Engineering, University of California, Berkeley, CA 94720, USA

ARTICLE INFO

Article history:

Received 31 August 2011

Revised 2 November 2011

Accepted 3 November 2011

Available online 15 November 2011

Edited by: David Burr

Keywords:

Human cortical bone

Toughness

Mixed-mode loading

ABSTRACT

Bone is generally loaded under multiaxial conditions *in vivo*; as it invariably contains microcracks, this leads to complex mixed-mode stress-states involving combinations of tension, compression and shear. In previous work on the mixed-mode loading of human cortical bone (using an asymmetric bend test geometry), we found that the bone toughness was lower when loaded in far-field shear than in tension (opposite to the trend in most brittle materials), although only for the *transverse* orientation. This is a consequence of the competition between preferred mechanical vs. microstructural crack-path directions, the former dictated by the direction of the maximum mechanical “driving force” (which changes with the mode-mixity), and the latter by the “weakest” microstructural path (which in human bone is along the osteonal interfaces or cement lines). As most microcracks are oriented longitudinally, we investigate here the corresponding mixed-mode toughness of human cortical bone in the *longitudinal* (proximal–distal) orientation using a “double cleavage drilled compression” test geometry, which provides a physiologically-relevant loading condition for bone in that it characterizes the toughness of a longitudinal crack loaded in far-field compression. In contrast to the transverse toughness, results show that the longitudinal toughness, measured using the strain-energy release rate, is significantly higher in shear (mode II) than in tension (mode I). This is consistent, however, with the individual criteria of preferred mechanical vs. microstructural crack paths being commensurate in this orientation.

Published by Elsevier Inc.

Introduction

Under physiological conditions, bones invariably experience multiaxial loads during routine activities as well as traumatic events that can cause fractures [1,2]. As human cortical bone contains a distribution of microcracks [3], it is important to understand how bone's resistance to fracture is affected by the presence of such complex loads, which can result in various combinations of mode I (tension), mode II (in-plane shear), and/or mode III (out-of-plane shear) displacements and hence stress intensities¹ at the tips of

these cracks. The three modes of crack displacements are shown in Fig. 1.²

Even though such mixed-mode fracture is a physiologically relevant scenario in cortical bone, the vast majority of fracture mechanics studies on the toughness of bone have been performed in mode I as this generally represents the loading condition which yields the “worst-case” fracture toughness in most materials, i.e., the pure mode I fracture toughness is invariably the lowest. This is illustrated in Fig. 2 where the toughness, expressed in terms of the critical strain-energy release rate, G_c , is plotted for several materials, specifically alumina, zirconia and wood³ [4,5], as a function of the phase angle, Ψ , which is defined as the inverse tangent of the mode-mixity, K_{II}/K_I , i.e., $\Psi = \tan^{-1} [K_{II}/K_I]$. The parameter, G_c , can be regarded here as the mixed-mode fracture toughness, i.e., the critical crack-driving force under multiaxial conditions; it is related to the

* Corresponding author at: Department of Materials Science and Engineering, University of California, Berkeley, CA 94720, USA. Fax: +1 510 643 5792.

E-mail address: RO Ritchie@lbl.gov (R.O. Ritchie).

¹ The stress-intensity factor K characterizes the local distribution of stress and displacement in the vicinity of a sharp crack in a linear-elastic solid. It is determined by $K = Y\sigma_{app}(\pi a)^{1/2}$ where σ_{app} is the applied stress, a is the crack length, and Y is a function (of order unity) of crack size and geometry. Stress-intensity factors can be defined for each displacement mode, namely K_I , K_{II} , and K_{III} . (Mode III is included for completeness but is not addressed, nor pertinent, to this study). Alternatively, the crack-driving “force” can be expressed in terms of the strain-energy release rate, G , defined as the change in potential energy per unit increase in crack area. Critical values of these K and G parameters at fracture are measures of the material's fracture toughness.

² To avoid confusion, we use the terms “mode I” and “mode II” to refer to conditions of local tensile and shear displacements, respectively, at the crack tip, while the corresponding terms “tension”, “shear” and “compression” refer to the globally applied (far-field) loading.

³ Anisotropic materials such as bone and wood clearly show more complex behavior, as discussed below.

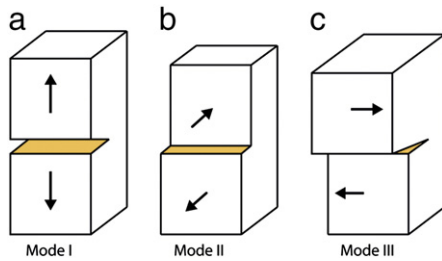


Fig. 1. Schematic illustration of the three different modes of crack displacements. (a) mode I (tension), (b) mode II (in-plane shear), and (c) mode III (out-of-plane shear). Stress-intensity factors can be defined for each, namely K_I , K_{II} , and K_{III} . This study is focused on the toughness of bone with combinations of mode I and mode II at the crack tip.

stress-intensity based toughnesses through the following expression [6]:

$$G_c = \frac{K_{Ic}^2}{E'} + \frac{K_{IIc}^2}{E'} + \frac{K_{IIIc}^2}{2\mu}, \quad (1)$$

where K_{Ic} , K_{IIc} and K_{IIIc} are, respectively, the mode I, II, and III fracture toughness values; E' is the appropriate elastic modulus (given by the Young's modulus E , in plane stress and $E/(1-\nu^2)$ in plane strain, where ν is Poisson's ratio); and μ is the shear modulus. Conditions of pure mode I are represented by a phase angle of 0° , whereas for pure mode II shear the phase angle is 90° .

Although the results in Fig. 2 showing a progressive elevation in fracture toughness with increasing mode II (shear) stress intensities are typical for most materials and have been reported [7,8] in the past for both the longitudinal and transverse orientations in bone⁴, recent results over a wider range of phase angles (also plotted in Fig. 2) have clearly shown that the fracture toughness of human cortical bone in the transverse orientation actually decreases with increasing mode-mixity (as in wood [4]), indicating that resistance to fracture in this orientation is lower in mode II rather than in mode I [9,10].⁵ Indeed, the value of the G_c toughness in pure mode II was found to be only 25% of that measured in mode I.

The fact that the toughness measured in mode I may not be the lower-bound highlights the need to characterize the fracture resistance of bone under more realistic mixed-mode conditions. As most microcracks are oriented close to the long axis of the bone [3], it is the focus of this work to expressly characterize the mixed-mode fracture toughness of hydrated human cortical bone in this longitudinal (proximal–distal) orientation. To achieve this, we use a geometry new to the bone community, that of the double cleavage drilled compression (DCDC) test geometry, which axially loads a sample containing a longitudinal crack in applied far-field compression. This geometry provides a physiologically realistic loading scenario, is easy to use, and further enables the evaluation of bone toughness under mixed-mode loading conditions.

⁴ In the longitudinal (proximal–distal) orientation under study here, the original crack is parallel to the direction of the osteons, i.e., along the long axis of the bone. In the transverse orientation, conversely, the original crack is perpendicular to the osteonal direction (see the inset of Fig. 2).

⁵ The discrepancy between these recent results [9,10] and the older data of Feng et al.'s [7] that showed an increasing transverse toughness with increasing mode-mixity is that Feng et al. used test samples with side-grooves (to nearly half thickness) to constrain the crack to take a straight path. This, however, is completely artificial and suppresses one of the main toughening mechanisms in bone in the transverse orientation, that of major crack-path tortuosity caused by deflection and twisting of the crack as it encounters the cement lines [9,11]. We therefore consider Feng et al.'s [7] results to be spurious in that they do not reflect *in vivo* conditions.

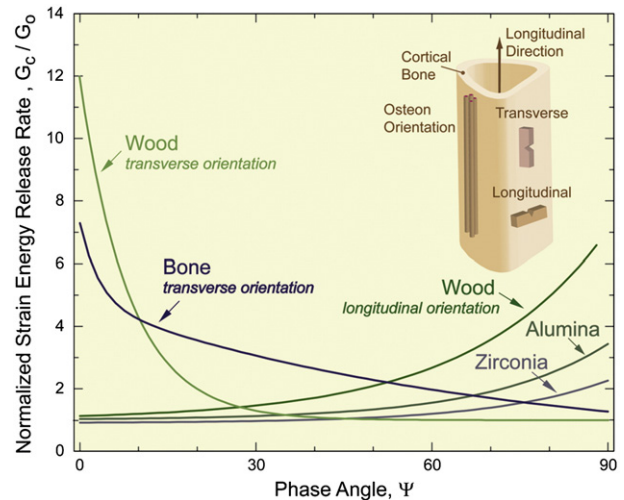


Fig. 2. Variation in the fracture toughness of various materials with mode-mixity. Plotted are the fracture toughness values for several materials, expressed as the critical strain-energy release rate, G_c , normalized by the lower-bound strain-energy release rate, G_0 , as a function of the mode-mixity, defined in terms of the phase angle, $\Psi = \tan^{-1} [K_{II}/K_I]$, where K_I and K_{II} are, respectively, the mode I and mode II stress-intensity factors. (Note: $\Psi = 0^\circ$ for pure local tension (mode I) and 90° for pure local shear (mode II)). For alumina and zirconia, as well as wood in the longitudinal orientation [4,5], the mixed-mode toughness can be seen to increase with increasing mode-mixity, i.e., with an increasing proportion of local shear (mode II) loading; this behavior is commonly seen for most materials. However, for the transverse orientation, recent results on wood and human cortical bone [9] are found to display exactly the opposite behavior; this implies that bone is “weaker” in mode II rather than in mode I in this orientation. The inset shows a schematic of the transverse and longitudinal orientations relevant to cortical bone together with the orientation of the osteons, the boundaries of which provide preferred “microstructurally weak” paths for cracking.

Experimental methods

A fresh frozen human cadaveric femur from a diabetic male of 56 years of age was used in this study. From the diaphysis of the femur, 17 beams of length $L \sim 39.8$ – 41.4 mm with a rectangular cross-section of width ~ 4.0 – 4.3 mm and thickness ~ 2.9 – 4.5 mm were sectioned from the cortical bone with an electric saw, such that $L/w = 20$, where w is the half width of the sample. These beams were cut in the longitudinal (proximal–distal) orientation such that the osteons were nominally oriented parallel to the long axis of the sample (Fig. 3a). All samples were stored in Hanks' Balanced Salt Solution (HBSS) prior to machining and/or testing.

Measurement of the mixed-mode toughness of human cortical bone in the longitudinal orientation requires a sample geometry that applies multiaxial loads to the crack tip. Although many mixed-mode sample geometries have been developed to characterize the effect of combined mode I and mode II loading [12–16], few provide (nominally) realistic loading scenarios for bone. We utilize here, however, the double cleavage drilled compression (DCDC) geometry [14,16], which involves the far-field compression loading of a longitudinally cracked sample. Depending on the locations of the longitudinal crack and the hole, a range of mode mixities from $\Psi = 0$ to 64° can be achieved. With this geometry, combinations of mode I and mode II displacements can be generated at the crack tip by tuning the position of the hole and the crack while a compressive load is applied axially. Specifically, a pure mode I condition ($\Psi = 0^\circ$) arises when the hole and the crack are aligned with the center line of the sample (Fig. 3a), whereas combinations of mode I+II conditions ($0^\circ < \Psi \leq 64^\circ$) occur at the crack tip by varying the offset, b , of the hole and/or the longitudinal crack with respect to the centerline of the sample (Fig. 3b, c).

To create the DCDC geometry, a hole with a radius of $r \sim 0.50$ – 0.75 mm was drilled in each sample. To prepare mode I samples,

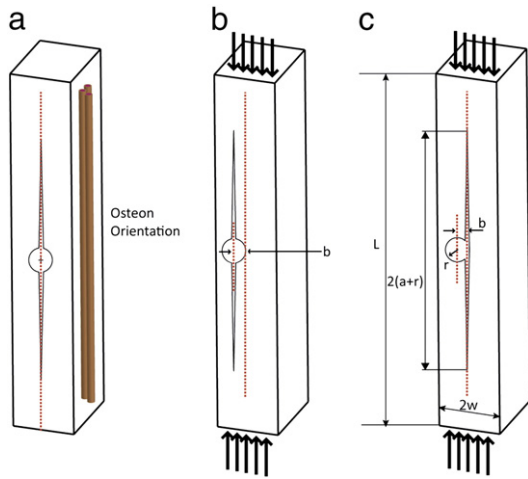


Fig. 3. The DCDC geometry provides a realistic physiological scenario in that a longitudinal crack in the test sample is loaded in far-field compression. (a) With the longitudinal crack emanating from the central hole both aligned directly with the centerline of the sample, a pure mode I (tensile) loading is achieved at the crack tip ($\Psi=0^\circ$). Osteons are nominally oriented parallel to the long axis of the sample. (b) A mixed-mode condition occurs when the hole and the crack are offset from the centerline of the sample (depicted as the dotted line) by an amount b ; depending upon its location, various combinations of mode I (tension) and mode II (shear) can be generated at the crack tip corresponding to phase angles (Ψ) below 20° . (c) Displacing only the hole from the centerline produces phase angles above 20° . In the diagram, L is the length of the sample; B and w are its thickness and half width, respectively; r is the radius of the hole; and $2(a+r)$ is the full length of the crack.

the axis of the hole and the crack were aligned with the sample's centerline, i.e., b/r equal to zero (see Fig. 3a). To prepare mixed-mode samples with a phase angle between 0 and 20° , the hole with the longitudinal crack emanating from its center was offset with a b/r ratio between ~ 0.4 and 0.75 (see Fig. 3b). To create mixed-mode conditions for phase angles between 20° and 64° , the axis of the hole was displaced by $b/r \sim 0.15$ – 0.5 with a longitudinal crack along the centerline of the sample (see Fig. 3c). Four mode I samples and thirteen mixed-mode samples were prepared.

The DCDC geometry requires a long crack with the following length requirements:

$$\frac{w}{r} \leq \frac{a}{r} \leq 15\text{mm}, \quad (2)$$

where a is the crack length. The crack was introduced with an electric saw using a small, thin saw blade; the resulting notch was then sharpened by polishing the root of the crack with a razor blade irrigated with $1\text{-}\mu\text{m}$ diamond suspension to give a final crack with a length in the range of $13.4\text{ mm} \leq 2(a+r) \leq 18.0\text{ mm}$ with a reproducible root radius of $\sim 25\text{ }\mu\text{m}$ (this is at least an order of magnitude smaller than the length of typical microcracks in bone). Samples were stored in HBSS for at least 12 h prior to testing.

To measure the fracture toughness, both mode I and mixed-mode samples were loaded in far-field compression using an electro-servo-hydraulic MTS 831 testing machine (MTS Systems Corp., Eden Prairie, MN) at a displacement rate of $1\text{ }\mu\text{m/s}$ in 37°C HBSS. As the sample was loaded, the applied load and the displacement of the load frame were recorded. Using measurements of the sample's geometry and the peak load attained during testing, the critical value of the crack-driving force, G_c , was computed in terms of the critical value of the strain-energy release rate from the solutions for the DCDC geometry given in refs. [14,16]. For the mode I toughness, where the crack and hole are aligned with the centerline of the DCDC sample, the

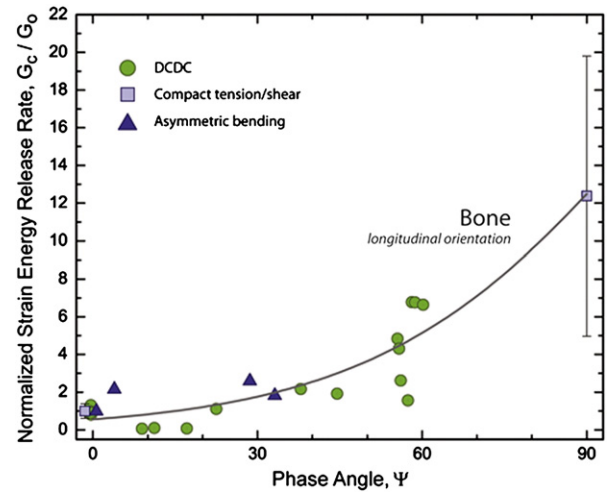


Fig. 4. The toughness of hydrated human cortical bone tested in 37°C HBSS in the longitudinal orientation as a function of mode-mixity. In contrast to behavior in the transverse orientation (Fig. 2), mixed-mode fracture toughness values in the longitudinal orientation, assessed in terms of the critical strain-energy release rate, G_c , and normalized by the lower-bound strain-energy release rate, G_0 (at $\Psi=0^\circ$), progressively increase with increasing mode-mixity. Based on the current data on DCDC samples, the results of Zimmermann et al. [9] on asymmetric bending samples, and those of Norman et al. [8] on compact-tension/shear samples, human cortical bone in this orientation appears to be an order of magnitude tougher in pure shear as compared to pure tension.

strain-energy release rate is given in terms of the applied (far-field) compressive stress σ_{app} [14]:

$$G = \frac{(\sigma_{\text{app}}^2 \pi r) \left[\frac{w}{r} + \left(\frac{0.235w}{r} - 0.259 \right) \frac{a}{r} \right]^{-2}}{E'}, \quad (3)$$

where E' is the appropriate elastic modulus (given by $E/(1-\nu^2)$ for plane strain, where ν is Poisson's ratio and E is Young's modulus); in this study, E' was taken to be 20 GPa ⁶. Expressions for G for the mixed-mode DCDC geometries (Fig. 3b,c) are dependent on the placement of the offset hole and/or longitudinal crack [14,16]. For mixed-mode samples with a phase angle between 0 and 20° (Fig. 3b), the strain-energy release is given in terms of the applied (far-field) compressive stress σ_{app} :

$$G = \frac{(\sigma_{\text{app}}^2 \pi r) \left[d_0 + \frac{d_1 a}{r} + \left(\frac{d_2 w}{r} - d_3 \right) \frac{a}{r} \right]^{-2}}{E'}, \quad (4)$$

where the dimensionless coefficients, d_i , depend on the offset of the hole relative to its radius (i.e., b/r). These coefficients are tabulated in ref. [16]. For mixed-mode samples with a phase angle between 20° and 64° (Fig. 3c), the strain-energy release is given in terms of the applied (far-field) compressive stress σ_{app} :

$$G = \frac{(\sigma_{\text{app}}^2 \pi r) \left[c_0 + \frac{c_1 a}{r} + \frac{c_2 w}{r} + c_3 \left(\frac{a}{r} \right) \left(\frac{w}{r} \right) + c_4 \left(\frac{a}{r} \right)^2 + c_5 \left(\frac{w}{r} \right)^2 \right]^{-2}}{E'}, \quad (4)$$

⁶ Note that in keeping with virtually all fracture toughness measurements to date on bone, these analyses pertain strictly to isotropic materials, which must be considered as a limitation to most fracture mechanics analyses of bone. In the present study though, we have utilized the appropriate mechanical properties, specifically the elastic modulus, for the particular orientation of the bone in question.

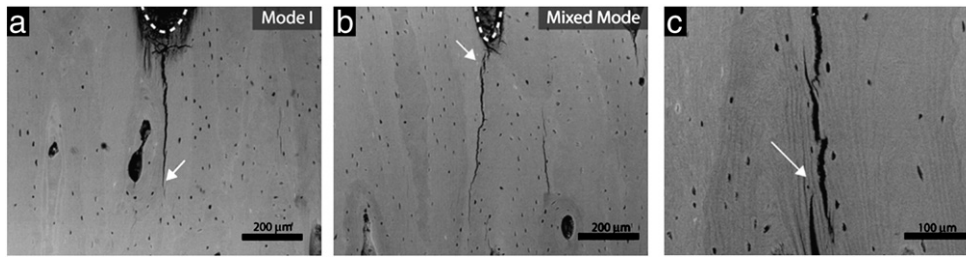


Fig. 5. Scanning electron microscopy images of crack trajectories in hydrated human cortical bone in the longitudinal orientation. (a) For crack propagation out from the starter crack under mode I ($\Psi = 0^\circ$) loading, the crack follows the expected maximum K_I (straight) path perpendicular to the direction of the maximum tensile stress. (b) Under the mixed-mode case ($\Psi = 60^\circ$), the crack follows an initially angled deflected path. (c) Note the formation of parallel microcracks, shown by the white arrows (also in (a) and (b)) adjacent to the main crack and the “uncracked-ligament” bridges that these create. These cracks initiate along the weak interfaces, which are principally the cement limits and are thus aligned nominally along the long axis of the bone. The white dotted line delineates the tip of the initial starter crack.

where c_i are dimensionless coefficients dependent on b/r ; these are also tabulated in ref. [16].

After testing, the samples were ground with successively finer grit from 400 to 1200 grit prior to final polishing with a 1- μm and then a 0.05- μm diamond suspension. Characterization of the crack path was performed in an Hitachi S-4300SE/N environmental scanning electron microscope, eSEM (Hitachi America, Pleasanton, CA) operating in back-scattered electron mode at an accelerating voltage of 25 kV with a pressure of 35 Pa.

Results

Results from the DCDC samples showing the mixed-mode fracture toughness of HBSS-hydrated human cortical bone in the longitudinal orientation are shown in Fig. 4 in terms of the critical strain-energy release rate, G_C , as a function of the phase angle, Ψ . Data are compared with our previous study using asymmetric bending samples [9] and earlier work by Norman et al. [8] using compact-tension/shear samples (mode I and mode II).

From the current study with DCDC samples, the average critical strain-energy release rate was 3.28 ± 0.72 N/m for mode I ($\Psi = 0^\circ$) conditions, which is significantly lower (by a factor of almost five) than the G_C of 15.75 ± 6.92 N/m measured under mixed-mode conditions with $\Psi = 55.5\text{--}60.2^\circ$ ($p = 0.0066$).

The general trend shown in Fig. 4, based on the results of three different investigations using four quite distinct specimen geometries, is that the fracture toughness of human cortical bone in the longitudinal orientation increases significantly with increasing mode-mixity, specifically with an increasing proportion of shear (mode II) to tensile (mode I) displacements; this is quite distinct to the observed behavior in the transverse orientation shown in Fig. 2.

Corresponding images, taken in the eSEM of the path of the crack as it emanates from the starter notch, are shown in Fig. 5a, b for mode I ($\Psi = 0^\circ$) and mixed-mode ($\Psi = 60^\circ$) loading. In mode I, the crack can be seen to grow in the same direction as the starter crack (indicated by the dotted line), i.e., along the path of maximum K_I (Fig. 5a), in contrast to mixed-mode conditions where the crack initially grows at an angle to this direction (Fig. 5b). In both cases, parallel microcracks, which initiated primarily along the osteonal interfaces (cement lines, lamellae, etc.), can be seen to have formed adjacent to the main crack, with small “uncracked-ligament” bridges in between where these cracks attempt to link up (see Fig. 5c). Such cracking morphologies are very characteristic of longitudinal fractures in human cortical bone [9,11].

Discussion

As bones are subjected physiologically to complex multiaxial loading conditions, combinations of tension (mode I) and shear (modes II or III) will be generated at the tips of any pre-existing cracks. In

fracture mechanics terms, an appropriate measure of bone's fracture resistance should therefore involve an assessment of the mixed-mode fracture toughness, particularly because mode I toughness values, which are invariably quoted, are not always worst-case for bone. In this work, we present a test specimen, the double cleavage drilled compression (DCDC) geometry, which is new to the biomechanics literature, and which can be used to evaluate the mixed-mode toughness of bone, in particular for the longitudinal orientation. This geometry has the special advantage of representing a nominally realistic loading configuration for bone in that it evaluates a longitudinal crack in far-field compression; with this geometry, phase angles varying from 0° (mode I) to 64° (mode I + II) can be obtained.

Using the DCDC specimen, we find that the fracture toughness of human cortical bone in 37 °C HBSS increases progressively with increasing mode-mixity (Fig. 4), consistent with previous results on bone using asymmetric bend [9] and compact tension/shear [8] specimens (mode I and mode II). Specifically in terms of the strain-energy release rate, the longitudinal toughness in mode II is roughly an order of magnitude higher than in mode I. Although this is the expected behavior for many materials, including longitudinally-oriented wood (Fig. 2) [4,5], this result is in complete contrast to the effect of multi-axial loading on the transverse fracture properties of bone (and wood) where the toughness progressively decreases with increasing mode-mixity [9,10] (Fig. 2). Essentially bone is tougher in mode II (shear) longitudinally yet tougher in mode I (tension) in the transverse orientation.

While seemingly contradictory, these results are completely consistent with the notion that the toughness of bone is strongly associated with the path of the crack in relation to the bone-matrix microstructure. Microstructurally, there are preferred crack paths in human cortical bone which are aligned along its long axis. Indeed, bone is far easier to split than to break [9,11]. The long axis is the nominal orientation of the secondary osteonal structures which consist of a central vascular cavity, the Haversian canal, surrounded concentrically by lamellae [17]. Prior to deposition of the lamellae during the formation of the osteons, a roughly 5- μm -thick layer called the cement line is deposited [18,19], which separates the osteon from the surrounding interstitial lamellae. These cement lines represent hyper-mineralized interfaces [20]⁷, and as such provide preferred sites for microcrack formation; indeed, some 99% of all microcracks have been reported to be aligned within 25° of the osteonal direction [3]. They therefore serve as a preferential low-energy microstructural path for a crack to follow.⁸

⁷ There has been some controversy in the literature about the nature of the cement lines in bone. Early work suggested that they were mineral-deficient [21], although we believe that the recent studies have clearly demonstrated their hyper-mineralized character [20,22].

⁸ The interaction of these microcracks with the main growing crack also provides a major source of toughening in bone through the formation of “uncracked-ligament” bridging and crack deflection mechanisms [11, 23, 24].

However, the actual path of a crack, and in turn the toughness, depends not simply on the microstructure but also on the applied loading. Understanding the directionality of the applied driving force is another key in mixed-mode tests. A mode I (tensile) stress intensity at the crack tip of an isotropic homogeneous material would cause the crack to follow a straight path, while an in-plane mode II (shear) stress intensity would cause a roughly 74° deflection of the crack in the same material (with deflections between 0 and 74° for different combinations of mode I and mode II). The mixed-mode driving force causes deflections in the crack path because cracks tend to follow the path wherein $K_{II} = 0$, i.e., a path subject to the maximum tensile stresses where K_I is at a maximum; this is essentially equivalent to a path of maximum G and is termed the preferred direction of the mechanical driving force. Accordingly, the actual crack trajectory is the result of a competition between these two “drivers”: the direction of the maximum crack-driving “force”, which is a function of the nature and mixity of the applied loading, and the path of “weakest” microstructural resistance, which in bone, as we have stated, is along its long axis. It is a general phenomenon in materials that where these two criteria are commensurate the toughness tends to be low, whereas where they are incommensurate, a much higher toughness results [9,10,25].

When bone is loaded such that cracks in the longitudinal orientation locally experience tension (mode I), the preferred mechanical and microstructural paths coincide (the two crack-path criteria are commensurate) along the longitudinal orientation. This is the reason that the mode I toughness in the longitudinal orientation is a lower-bound (at $\Psi = 0^\circ$). Increasing the mode-mixity then acts to progressively diverge these preferred crack paths such that the mixed-mode toughness increases with increasing Ψ (Fig. 4). Similarly, when cracks in the transverse orientation locally experience shear (mode II), the two crack-path criteria are again commensurate, and the lower-bound toughness is achieved at $\Psi = 90^\circ$. Now decreasing the mode-mixity causes these preferred crack paths to become divergent with the result that the mixed-mode toughness now increases with decreasing Ψ (Fig. 2).

Finally, we note that as most actual bone fractures in humans are rough (multi-orientated) mixed-mode failures, the mixed-mode fracture toughness is the most appropriate means to assess the fracture resistance of bone; in this regard, the DCDC test specimen presented here represents a simple, physiologically relevant, sample to evaluate this toughness over a range of mode-mixities.

Conclusions

Based on an experimental study of the fracture toughness of human cortical bone in 37 °C Hanks' Balanced Salt Solution under combined mode I (tension) and mode II (shear), specifically using the double cleavage drilled compression (DCDC) test geometry to evaluate the longitudinal fracture resistance, the following conclusions can be made:

1. The DCDC test geometry, where a longitudinally cracked specimen is loaded axially in far-field compression, provides a convenient way to evaluate the toughness of bone in the longitudinal orientation over a range of phase angles ($\Psi = \tan^{-1} K_{II}/K_I$) from 0 to 64°. As most *in vivo* microcracks in bone are aligned nominally along the long axis of the bone, the DCDC geometry provides a physiologically more relevant loading mode than most other fracture mechanics tests used to assess bone toughness.
2. Whereas the mixed-mode fracture toughness of bone decreases with increasing mode-mixity (increasing phase angle) in the transverse orientation, we find that the bone toughness increases with increasing mode-mixity in the longitudinal (proximal–distal) orientation. In both instances, the difference in the toughness for pure tension ($\Psi = 0^\circ$) vs. pure shear ($\Psi = 90^\circ$) is about a half to one order of

magnitude. This implies that bone containing a longitudinal crack is tougher in mode II (shear) rather than in mode I (tension) conditions, whereas bone containing a transverse crack is tougher in mode I (tension) than in mode II (shear).

3. This orientation-dependent difference in the variation in bone toughness with mode-mixity is consistent with the notion that the toughness is a marked function of the path of the crack with respect to the bone-matrix structure. The crack path in turn results from a competition between the preferred mechanical path, which is a function of the applied loading in dictating the direction of maximum strain-energy release rate (or where $K_{II} = 0$), and the preferred microstructural path with “weakest” resistance, which in human cortical bone is along its long axis, specifically along the cement lines.
4. Where these two criteria are commensurate, i.e., the preferred mechanical and microstructural paths converge or coincide, as for pure mode I fracture in the longitudinal orientation or for pure mode II fracture in the transverse orientation, the toughness is low.
5. Where these two criteria are incommensurate, i.e., the two paths diverge, as with increasing mode-mixity in the longitudinal orientation or decreasing mode-mixity in the transverse orientation, the toughness is increased.
6. As most *in vivo* bone fractures derive from complex physiological multiaxial loads, we believe that any assessment of the fracture resistance of bone must involve measurements of the mixed-mode fracture toughness over a range of mode-mixities.

Acknowledgments

This work was supported by the National Institutes of Health (NIH/NIDCR) under grant no. 5R01 DE015633 to the Lawrence Berkeley National Laboratory (LBNL). The authors wish to thank Dr. Tony Tomsia and Brian Panganiban for their assistance with the study, and Professor Tony Keaveny and Mike Jekir, of the Mechanical Engineering Department at the University of California, Berkeley, for allowing us to use their bone machining facilities.

References

- [1] Burr DB, Milgrom C, Fyhrie D, Forwood M, Nyska M, Finestone A, et al. In vivo measurement of human tibial strains during vigorous activity. *Bone* 1996;18:405–10.
- [2] Carter DR. Anisotropic analysis of strain rosette information from cortical bone. *J Biomech* 1978;11:199–202.
- [3] Wasserman N, Brydges B, Searles S, Akkus O. In vivo linear microcracks of human femoral cortical bone remain parallel to osteons during aging. *Bone* 2008;43:856–61.
- [4] Jernkvist LO. Fracture of wood under mixed mode loading: II. Experimental investigation of Picea abies. *Eng Fract Mech* 2001;68:565–76.
- [5] Singh D, Shetty DK. Fracture toughness of polycrystalline ceramics in combined mode I and mode II loading. *J Am Ceram Soc* 1989;72:78–84.
- [6] Irwin GR. Analysis of stresses and strains near the end of a crack traversing a plate. *J Appl Mech* 1957;24:361–4.
- [7] Feng Z, Rho J, Han S, Ziv I. Orientation and loading condition dependence of fracture toughness in cortical bone. *Mater Sci Eng C* 2000;11:41–6.
- [8] Norman TL, Nivargikar SV, Burr DB. Resistance to crack growth in human cortical bone is greater in shear than in tension. *J Biomech* 1996;29:1023–31.
- [9] Zimmermann EA, Launey ME, Barth HD, Ritchie RO. Mixed-mode fracture of human cortical bone. *Biomaterials* 2009;30:5877–84.
- [10] Zimmermann EA, Launey ME, Ritchie RO. The significance of crack-resistance curves to the mixed-mode fracture toughness of human cortical bone. *Biomaterials* 2010;31:5297–305.
- [11] Koester KJ, Ager JW, Ritchie RO. The true toughness of human cortical bone measured with realistically short cracks. *Nat Mater* 2008;7:672–7.
- [12] Atkinson C, Smelser RE, Sanchez J. Combined mode fracture via the cracked Brazilian disk test. *Int J Fract* 1982;18:279–91.
- [13] He MY, Hutchinson JW. Asymmetric four-point crack specimen. *J Appl Mech* 2000;67:207–9.
- [14] He MY, Turner MR, Evans AG. Analysis of the double cleavage drilled compression specimen for interface fracture energy measurements over a range of mode mixities. *Acta Metall Mater* 1995;43:3453–8.

- [15] Charalambides PG, Cao HC, Lund J, Evans AG. Development of a test method for measuring the mixed-mode fracture resistance of bimaterial interfaces. *Mech Mater* 1990;8:269–83.
- [16] Lardner TJ, Chakravarthy S, Quinn JD, Ritter JE. Further analysis of the DCDC specimen with an offset hole. *Int J Fract* 2001;109:227–37.
- [17] Weiner S, Wagner HD. The material bone: structure mechanical function relations. *Annu Rev Mater Sci* 1998;28:271–98.
- [18] Currey JD. *Bones: structure and mechanics*. Princeton, NJ: Princeton University Press; 2002.
- [19] Schaffler MB, Burr DB, Frederickson RG. Morphology of the osteonal cement line in human bone. *Anat Rec* 1987;217:223–8.
- [20] Skedros JG, Holmes JL, Vajda EG, Bloebaum RD. Cement lines of secondary osteons in human bone are not mineral-deficient: new data in a historical perspective. *Anat Rec A* 2005;286A:781–803.
- [21] Burr DB, Schaffler MB, Frederickson RG. Composition of the cement line and its possible mechanical role as a local interface in human compact-bone. *J Biomech* 1988;21:939–45.
- [22] Skedros JG, Durand P, Bloebaum RD. Hypermineralized peripheral lamellae in primary osteons of deer antler: potential functional analogs of cement lines in mammalian secondary bone. *J Bone Miner Res* 1995;10:S441.
- [23] Launey ME, Buehler MJ, Ritchie RO. On the mechanistic origins of toughness in bone. *Annu Rev Mater Res* 2010;40:25–53.
- [24] Nalla RK, Kinney JH, Ritchie RO. Mechanistic fracture criteria for the failure of human cortical bone. *Nat Mater* 2003;2:164–8.
- [25] Ritchie RO, Cannon RM, Dalgleish BJ, Dauskardt RH, McNaney JM. Mechanics and mechanisms of crack growth at or near ceramic-metal interfaces: interface engineering strategies for promoting toughness. *Mater Sci Eng, A* 1993;166:221–35.